

Transplantation Publish Ahead of Print

DOI: 10.1097/TP.0000000000002773

The effects of an IL-21 receptor antagonist on the alloimmune response in a humanized mouse skin transplant model

Kitty de Leur, MSc^{1,2}, Franka Luk, PhD¹, Thierry P.P. van den Bosch, PhD³, Marjolein Dieterich, BSc¹, Luc J.W. van der Laan, PhD², Rudi W. Hendriks, PhD⁴, Marian C. Clahsen - van Groningen, MD, PhD³, Fadi Issa, MD, PhD⁵, Carla C. Baan, PhD¹, Martin J. Hoogduijn, PhD¹

¹The Rotterdam Transplant Group, Department of Internal Medicine, ²Department of Surgery, ³Department of Pathology, ⁴Department of Pulmonary Medicine, Erasmus MC, University Medical Center Rotterdam, The Netherlands, ⁵Nuffield Department of Surgical Sciences, Transplantation Research Immunology Group, University of Oxford, United Kingdom

Corresponding author: Martin Hoogduijn, Erasmus MC, Room Na-516, Wytemaweg 80, 3015 CN Rotterdam, The Netherlands. Email: m.hoogduijn@erasmusmc.nl,

Running title: α IL-21R in a humanized skin transplant mouse model

Author contributions:

- KdL participated in research design, performing the research, data analysis and writing of the article.
- FL participated in research design, performing the research, data analysis and revision of the article.
- TPPvdB provided technical help and revision of the article.
- MD provided technical help and revision of the article.
- LJWvdL participated in research design and revision of the article.

- RWH participated in research design and revision of the article.

- MCC-VG provided analytical tools and revision of the article

- FI provided technical help and revision of the article.

-CCB participated in research design and revision of the article.

-MJH participated in research design, performing the research, and writing of the article.

Disclosure: The authors of this manuscript declare no conflicts of interest as described by *Transplantation*.

Funding: This work was supported by a grant from the Erasmus MC, University Medical Center, Rotterdam, awarded by the Erasmus MC Medical research advisory committee (Mrace), grant no. 343564.

Abbreviations:

AMR = antibody-mediated rejection; CNIs = calcineurin inhibitors; DIEP = deep inferior epigastric artery perforator; DSA = donor-specific antibodies; FFPE = formalin fixed and paraffin-embedded; GVHD = graft-versus-host disease; H&E = hematoxylin and eosin; IL-21 = interleukin 21; IL-21R = interleukin 21 receptor; IP = intraperitoneal; Ker17 = keratin 17; NKT cell = natural killer T cell; SEM = standard error of the mean; STAT3 = signal transducer and activator of transcription 3; STAT3p = STAT3 phosphorylation; TCMR = T cell-mediated rejection; Tfh cell = T follicular helper cell; α IL-21R = anti-IL-21R.

Abstract

Background: Interleukin 21 (IL-21) is involved in regulating the expansion and effector function of a broad range of leukocytes, including T cells and B cells. In transplantation, the exact role of IL-21 in the process of allograft rejection is unknown. To further explore this, the aim of this study is to test the effect of an IL-21 receptor (IL-21R) blocking antibody on the early phase of allograft rejection in a humanized skin transplantation model in mice reconstituted with human T and B cells.

Methods: Immunodeficient Balb/c IL2 γ ^{-/-}Rag2^{-/-} mice were transplanted with human skin followed by adoptive transfer of human allogeneic splenocytes. Control animals were treated with a PBS vehicle while the other group was treated with a humanized anti-IL-21R antibody (α IL-21R).

Results: In the PBS treated animals, human skin allografts were infiltrated with lymphocytes and developed a thickened epidermis with increased expression of the inflammatory markers Keratin 17 (Ker17) and Ki67. In mice treated with α IL-21R, these signs of allograft reactivity were significantly reduced. Concordantly, STAT3 phosphorylation was inhibited in this group. Of note, treatment with α IL-21R attenuated the process of T and B cell reconstitution after adoptive cellular transfer.

Conclusion: These findings demonstrate that blockade of IL-21 signaling can delay allograft rejection in a humanized skin transplantation model.

Introduction

In transplantation, both short- and long-term allograft survival rates remain suboptimal, illustrating the need for new immunosuppressive agents.¹ In general, two types of renal allograft rejection are recognized: T cell-mediated rejection (TCMR) and antibody-mediated rejection (AMR). However, over the last years it has become clear that these two types of rejection responses are not as distinct as thought before. For example, in renal allograft biopsies, overlapping histological features of TCMR and AMR are often detected.² These rejections are characterized by allograft infiltration with both T and B cells as well as typical features of AMR, for instance the presence of de novo donor-specific antibodies (DSA).^{2,3} Unsurprisingly, these cases are not responsive to treatment strategies that target either TCMR or AMR alone.⁴

Adaptive alloimmune responses are established via three essential signals: 1) donor antigen presentation, 2) co-stimulation, and 3) upregulation of cytokine receptors and cytokine production, resulting in T and B cell activation. Current immunosuppressive treatments include calcineurin inhibitors (CNIs) that mainly target the T cell activation cascade. CNIs are unable to prevent B-cell driven AMR, which is normally addressed with B cell depleting therapies (*e.g.* rituximab and intravenous immunoglobulins). Therapies that target B cells are generally not used as maintenance therapy due to the side effect profile and their ineffectiveness in the prevention of TCMR.⁵ There is therefore a need for the development of immunosuppressive drugs with mechanisms of action that concurrently target T and B cells.

Interleukin-21 (IL-21) is a cytokine with a broad pattern of actions that affect the differentiation and function of several lymphoid cells.⁶ IL-21 binds to the IL-21 receptor (IL-21R), which forms a heterodimer with the common gamma chain (γ_c).⁷ Upon IL-21/IL-21R signaling, downstream JAK/STAT pathways are activated, of which signal transducer and

activator of transcription 3 (STAT3) is most predominant.⁶ IL-21 is produced by T follicular helper (Tfh) cells, Th17 cells, and natural killer T (NKT) cells and is important in the differentiation of functional Th17 and Tfh cells.^{6,8-10} For the CD8+ T cell compartment, IL-21 is a potent regulator of expansion and effector function and prolongs CD8+ T cell effector function in chronically infected hosts.¹¹⁻¹³ IL-21 is also crucial for naïve B cell differentiation to immunoglobulin-producing plasma cells after antigen recognition.^{14,15}

In solid organ transplantation, IL-21 is expressed during the process of rejection.¹⁶⁻¹⁸ Upon alloantigen stimulation, IL-21-secreting Tfh cells are present in the circulation at three months after renal transplantation and provide help to B cells for their differentiation towards plasmablasts.¹⁹ In addition, IL-21-expressing cells have been detected in renal rejection biopsies in acute TCMR, suggesting a local effect of IL-21 on cytotoxic CD8+ T cells in this type of rejection.²⁰ We have previously demonstrated that IL-21 is a key factor in the Tfh-cell dependent differentiation of alloantigen-stimulated B cells towards immunoglobulin producing plasmablasts.²¹ Anti-human IL-21 mAb treatment has also been shown to suppress graft-versus-host (GVH)-associated disease in a humanized murine model.²² Therefore, IL-21R blockade may affect the process of allograft rejection. In the present study, we investigated whether blockade of the IL-21/IL-21R pathway can inhibit the process of allograft rejection in the early phase.

To investigate the effect of human IL-21 signaling blockade on allograft rejection, we used a humanized skin transplant model in which immunodeficient Balb/c IL2 γ ^{-/-} Rag2^{-/-} mice are transplanted with human skin followed by adoptive transfer of human allogeneic splenocytes.²³ When setting up a humanized transplantation model in mice, a skin transplant model is the first choice, since it is relatively easy to obtain human skin and with one piece of human skin several experiments can be performed, which improves reproducibility. The process

of rejection of skin and a solid organ occurs via similar mechanism, making skin transplantation useful as a model for studying organ transplantation. Also, the use of the humanized skin transplant mouse model has proven successful in previous studies, in which the effect of several immune modulating therapies on skin inflammation was tested.²³⁻²⁶ In general, many of these compounds were shown to reduce the number of infiltrating T cells in the human skin.²³⁻²⁵ Using this model, we provide evidence for efficacy of IL-21 blockade in the control of the start of alloimmunity.

Material and methods

Mice

Balb/c IL2 γ ^{-/-} Rag2^{-/-} mice were bred and housed under specific pathogen free (SPF) conditions at the Erasmus Medical Center Experimental Animal Facility. The animals were housed in individually ventilated cages with *ad libitum* access to water and food and a 12 hour light-dark cycle. Mice were aged between 8 and 14 weeks at the time of the first experimental procedure. All experiments were approved by the Central Committee Animal Experiments Ethical Committee (license number AVD101002016635) and complied with the 1986 directive 86/609/EC of the Council of Europe.

Human skin

Waste material from human abdominal skin surgeries performed for deep inferior epigastric artery perforator (DIEP) flap reconstruction was anonymously obtained as approved by the Medical Ethical Committee of our center (MEC-2014-347). The humanized skin allograft transplant model is based on the model described by Issa et al.²³ Human skin grafts were retrieved from discarded abdominal skin using an electric dermatome (Zimmer, Utrecht, the Netherlands) in strips with a thickness of 200 μ m. From these strips, punch biopsies were taken

with a diameter of 1cm and kept in ice-cold PBS. The human skin grafts were all transplanted within 16 hours.

Human skin transplantation

Animals were subcutaneously injected with 0.05 mg/kg buprenorphine 0.5 hours prior and 12 hours after the surgery as analgesic. During the surgical procedure mice were kept under complete anesthesia via isoflurane inhalation (5% isoflurane initially followed by 2% to 2.5% with 1:1 air/oxygen mixture for maintenance) and the animals were kept warm on 37°C heating pads. The left dorsal flank of the mice was shaved and a circular piece of skin with a diameter of 1 cm was removed. A human skin graft was placed in the circular incision and stitched on the mouse with absorbable 5/0 suture (Safil®, B. Braun, Melsungen, Germany). The skin grafts were covered with a povidone-iodine nonadherent mesh (Johnson & Johnson, Amersfoort, the Netherlands) and pressure dressing wound and fixed with surgical tape. Ten days after the transplant procedure, the tape was removed under general anesthesia. Engraftment of the human skin graft was achieved 35 days after transplantation.

Preparation and adoptive transfer of human splenocytes

Human splenocytes were adoptively transferred 35 days after skin transplantation. Human splenocytes were obtained from a segment of the spleen from deceased kidney donors. Splenocytes were anonymously used for research purposes as described in article 13 of The Netherlands law of organ donation (Wet op Orgaandonatie, WOD). The spleen segments were disrupted and filtered through a 70µm cell strainer (Greiner Bio-one, Alphen a/d Rijn, The Netherlands) to obtain a single-cell suspension. Ficoll-paque (Amersham Pharmacia Biotech, Uppsala, Sweden) density gradient was used to collect mononuclear cells. An aliquot of splenocytes was used to isolate quiescent B cells via negative selection with CD43 MicroBeads

(Miltenyi Biotec, Bergisch Gladbach, Germany) (purities $\geq 90\%$). 25×10^6 splenocytes were mixed with 12.5×10^6 enriched B cells and suspended in 1mL of PBS. 35 days post skin transplantation 5×10^6 splenocytes and 2.5×10^6 enriched B cells were administered in 200 μ L PBS via intraperitoneal (IP) injection. The composition of T and B cells within the total infusion is depicted in Figure S1 (SDC, <http://links.lww.com/TP/B744>).

α IL-21R therapy

Humanized anti-IL-21R antibody (α IL-21R; also referred to as ATR-107) was kindly provided by Pfizer (New York, NY, USA). α IL-21R was administered via IP injection at a dose of 10mg/kg (recommended by Pfizer) on days 7, 14 and 21 after adoptive transfer of splenocytes.^{27,28} We started the administration of α IL-21R at day 7 after adoptive transfer in order to allow the splenocytes to first engraft and proliferate in order to reflect a healthy functioning immune system in the mice. α IL-21R antibody was infused three times to build up a significant level of antibody. PBS was used as a vehicle control.

Monitoring of the human skin graft

All mice were sacrificed 30 days after adoptive transfer of splenocytes in order to assess for evidence of skin rejection and inflammation at a single time point.²³

Flow cytometry

Human splenocytes were characterized by flow cytometry prior to adoptive transfer and from mouse blood and spleens 30 days after adoptive transfer. Cells were stained with antibodies specific for CD45 allophycocyanin (APC, BD), CD3 Brilliant Violet 510 (BV510, Biolegend, San Diego, CA, USA), CD4 Brilliant Violet 421 (BV421, Biolegend), and CD19 BV510 (Biolegend) and the viability marker 7-AAD (BD Biosciences).

In order to test whether α IL-21R effectively blocked the IL-21R, phosphorylation of STAT3 downstream of IL-21R was measured on CD4⁺ T cells by phospho-specific flow cytometry. Briefly, 200 μ l of blood from treated animals was stained with anti-CD3 BV510 (Biolegend, San Diego, CA, USA) and subsequently stimulated with recombinant human IL-21 (100 ng/ml, eBioscience, San Diego, CA, USA) or recombinant human IL-6 (100 ng/ml, PeproTech, Rocky Hill, NJ) for 15 minutes at 37°C. Cells were fixed for 10 minutes with Cytofix buffer (BD Biosciences, San José, CA, USA) at 37°C and permeabilized for 30 minutes in 1 ml 90% methanol at -20°C. Samples were then stained with anti-CD4 BV421 (Biolegend) and anti-pSTAT3 phycoerythrin (PE, BD Biosciences). All samples were measured on the FACSCanto II (BD Bioscience). Flow data were analyzed with Kaluza Analysis 5.1 software (Beckman Coulter, Brea, CA, USA).

Immunohistochemistry

Human skin grafts were removed at day 30 post adoptive cell transfer, formalin fixed and paraffin-embedded (FFPE), and processed following a standardized diagnostic protocol. Three μ m sections were cut and stained with hematoxylin and eosin (H&E). Immunohistochemical staining was performed on the Benchmark Ultra Stainer (Ventana, Basel, Switzerland). The following human mAbs were used: CD45 (Cell Marque, ref. V0000963, Rocklin, CA, USA), CD4 (Ventana, ref. 790-4423), CD8 (Ventana, ref. Y04591), CD20 (Ventana, ref. 790-2531), Keratin 17 (Ker17, Ventana, ref. G03114), Ki67 (Ventana, ref. 790-4286). Antibodies were incubated on the tissue sections for 30 minutes together with anti-rabbit or anti-mouse amplifiers. 3,3'-diaminobenzidine (DAB) was used as chromogen and sections were counterstained with hematoxylin. Analysis of the proportions of positive cells in a representative region of interest (including the epidermis and dermis) was performed by setting a fixed threshold followed by

calculating the positive area with the ImageJ software (NIH, <http://imagej.nih.gov/ij/>).

Measurement of the epidermal thickness

Epidermal thickness was measured at twenty consecutive points in H&E stained skin slides from which the mean epidermal thickness was calculated.

Statistical testing

GraphPad Prism 5 software (GraphPad Software Inc, San Diego, CA, USA, <http://www.graphpad.com>) was used for statistical analysis. Differences between unpaired groups were analyzed with the nonparametric Mann-Whitney test. A two-tailed p -value of <0.05 was considered to be statistically significant.

Results

α IL-21R antibody effectively blocks STAT3 phosphorylation

In order to assess the efficacy of α IL-21R to block IL-21R signaling, phosphorylation of STAT3 downstream of the IL-21R was measured on human T cells after adoptive transfer of human splenocytes in mice.²⁹ We tested the duration of efficient blockade of the IL-21R by measuring STAT3 phosphorylation at multiple time points after cellular infusion (Figure 1A). Mice were treated with the α IL-21R compound on days 7, 14 and 21 after adoptive transfer of human splenocytes and sacrificed at specific time points as depicted in Figure 1A ($n=1$ per time point). From day 42 after adoptive cellular transfer onwards the degree of human leukocyte chimerism within the blood was sufficient to perform the phospho-specific flow cytometry protocol to measure STAT3 phosphorylation (STAT3p). Whole blood was stimulated with IL-21 or IL-6 to induce STAT3p, followed by measurement of STAT3p. IL-6 stimulation was used as a positive control to induce STAT3p through bypassing the IL-21R. Figure 1B shows a representative flow cytometry plot of STAT3p staining. In this example, only 1.4% of CD3+ T cells were positive

for STAT3p after IL-21 stimulation in the presence of α IL-21R, compared with 65.9% in control animals that did not receive α IL-21R treatment. These cells responded to IL-6 stimulation thereby demonstrating that α IL-21R specifically targets the IL-21R. Cells from a vehicle treated animal expressed pSTAT3 after both IL-21 and IL-6 stimulation (Figure 1B). STAT3p remained suppressed until 49 days after the last infusion of α IL-21R (56 days after adoptive cellular transfer, Figure 1C). These data confirm efficient blockade of the IL-21 signaling pathway by α IL-21R treatment. For subsequent assays, we selected day 30 after adoptive cellular transfer for analysis to ensure IL-21R blockade.

α IL-21R mAb treatment delays rejection of the human skin

We next assessed the in vivo immunosuppressive effects of α IL-21R using a humanized mouse skin transplantation model. Mice were transplanted with a human skin allograft, reconstituted with human splenocytes, and subsequently treated with α IL-21R or PBS control as described above (Figure 2A). Mice were sacrificed at day 30 after adoptive cellular transfer for cross-sectional analysis by measurement of several hallmarks of skin rejection (Figure 2A). As expected, there was clear epidermal dyskeratosis in skin allografts from mice treated with PBS control. By contrast, mice that received α IL-21R treatment had markedly reduced evidence of epidermal damage (Figure 2B). Mean epidermal thickness was 370.9 μ m in animals treated with vehicle control (n=7) compared with 90.6 μ m in the α IL-21R-treated animals (n=8; $p<0.05$, Figures 2B and D). Infiltrates of mononuclear cells were detected in the human dermis of vehicle-treated animals. These infiltrates were absent in the human dermis of α IL-21R-treated animals (Figure 2C). Overall, these results show that the epidermal changes indicative of severe rejection that occur in vehicle-treated animals are delayed upon infusion of α IL-21R.

IL-21R blockade reduces lymphocyte infiltration in skin grafts

Human skin graft sections were stained by immunohistochemistry in order to phenotype the infiltrating mononuclear cells. The mean area of CD45 cell positivity in the dermis was 10.2% in the vehicle-treated animals compared to 2.2% in the α IL-21R-treated animals ($p<0.001$, Figure 3A). CD3 cell positivity correlated with the staining patterns for CD45, with 9.0% in the control group compared to 1.4% in the α IL-21R group ($p<0.05$, Figure 3B). CD4 cell positivity was 6.2% in the control group compared to 1.2% in the α IL-21R group ($p<0.05$, Figure 3C). CD8+ T cell numbers in the dermis and epidermis were low in both the control group and α IL-21R group (Figure 3D; $p<0.05$). Some CD8+ T cells resided within the epidermis in the control group animals while the CD4+ cells in these animals were mainly detected within the dermis (Figures 3C and D). CD20+ B cells were low within the control animals and barely detectable within the skin of α IL-21R-treated animals ($p=0.07$; Figure 3E).

IL-21R blockade reduces human skin inflammation markers

A consequence of the infiltration of mononuclear cells is the induction of local inflammation measured among others by increased cell proliferation (epidermal hyperplasia) and the activation of several keratins. In order to further assess this, we stained human skin graft sections with two epidermal proliferation markers. Upon injury, de novo production of Keratin 17 (Ker17) is associated with epidermal formation after skin injury.³⁰ Indeed, significantly higher levels of Ker17 were found in the vehicle-treated animals (mean positive area: 30.5%) compared to the α IL-21R-treated animals (mean positive area: 7.6%, $p<0.05$, Figure 4A). Proliferation of the epidermal cells was assessed by staining with the proliferation marker Ki67. The mean area of dividing epidermal cells of the vehicle-treated animals was 4.6% compared to 1.9% in the α IL-21R-treated animals ($p<0.05$, Figure 4B). Ki67 positive cells were mainly detected in the basal

layers of the epidermis, suggesting active hyperplastic activity in vehicle-treated animals. These findings suggest that IL-21R signaling contributes to the generation of a pro-inflammatory climate in the transplanted skin.

α IL-21R mAb treatment reduced human leukocyte engraftment

In order to investigate the mechanisms underlying decreased infiltration of lymphocytes and reduced inflammation of human skin grafts in α IL-21R-treated animals, we measured the numbers of lymphocytes in blood and spleen at different time points after adoptive transfer of human splenocytes in animals without a skin graft. The mean spleen weight (as a measure of cell engraftment) of two vehicle-treated animals was 319 mg at day 28 and 42 post splenocyte infusion (Figure 5A). Spleen weights of the α IL-21R-treated animals (at day 7, 14 and 21; protocol Figure 1A) were 38 mg at day 28 and increased to 169 mg at day 63 after cell infusion (Figure 5A). Absolute numbers of human CD45⁺ cells in the spleen of α IL-21R-treated animals also increased over time (Figure 5B).

In animals that received a skin graft, similar effects of α IL-21R mAb on human splenocyte engraftment were observed. The average spleen weight was 192 mg in the vehicle-treated animals compared to 42 mg in the α IL-21R-treated animals at day 30 after administration of splenocytes ($p < 0.001$, Figure 5C) and the proportions of human CD45⁺ within total viable lymphocytes were 22% in the vehicle group versus 0.8% in the α IL-21R group ($p < 0.01$, Figure 5C). In the blood we detected the same trend with a significant difference in human CD45⁺ lymphocyte chimerism levels when comparing the vehicle group and the α IL-21R group (mean: 3.6% versus 38% of total viable cells within the lymphocyte gate, respectively, $p < 0.001$, Figure 5D). The majority of the human CD45⁺ lymphocytes measured within the blood consisted of CD3⁺ T cells, with only minor amounts of CD19⁺ B cells (Figure 5E). This was observed for

both the vehicle-treated group and the α IL-21R-treated group and correlated with the low level of infiltrating human B cells in the human skin (Figure 3D). Overall, blockade of IL-21R signaling hampers engraftment of human lymphocytes in Balb/c IL2 γ ^{-/-} Rag2^{-/-} mice, suggesting an effect of IL-21R blockade on human leukocyte survival and proliferation.

Discussion

Evidence from previous studies presents a role for the pleiotropic cytokine IL-21 in the process of allograft rejection.^{16,17} Therefore, we hypothesized that blockade of the IL-21R in a humanized skin transplant model affects the early phase of rejection of the human skin. In the present study we demonstrate that rejection of a human skin graft occurs after adoptive transfer of human splenocytes in Balb/c IL2 γ ^{-/-} Rag2^{-/-} mice. In the presence of α IL-21R mAb, phosphorylation of STAT3 downstream the IL-21R is effectively blocked. Blockade of IL-21R signaling led to a significant inhibition of epidermal thickening, reduced infiltration of lymphocytes and decreased expression of inflammation markers Ker17 and Ki67 in human skin allografts.

The inhibition of human skin rejection through IL-21R blockade was accompanied by impaired engraftment of human lymphocytes. Blockade of IL-21R influenced the homeostatic proliferation of the infused cells and therefore their engraftment within the host. Indeed, previous studies present a role for IL-21 in lymphocyte homeostasis.³¹⁻³³ This impaired homeostatic proliferation may be a result of impaired cross talk between different lymphocyte subsets upon IL-21R blockade. For instance, IL-21R signaling is involved in the generation of Tfh cells and mediates Tfh cell help to activate B cell differentiation towards immunoglobulin producing plasma cells.^{21,34,35} Moreover, IL-21 is involved in sustaining CD8⁺ T cell responses, which is in line with the low levels of CD8⁺ T cells in the human skin that we detected in the presence of

α IL-21R.^{36,37} Furthermore, there is evidence that activation of Th17 cells is impaired by α IL-21R,¹⁰ which may contribute to the reduced allograft rejection upon IL-21R blockade. Despite the low engraftment of human lymphocytes following IL-21R inhibition, we succeeded to reach a level of human lymphocyte chimerism that is acknowledged in the literature as a reconstituted human lymphocyte system.^{38,39} To allow some degree of immune cell engraftment to occur, we decided to delay blockade of IL-21R signaling until day seven after infusion of human lymphocytes. Further delay of α IL-21R treatment or administration of higher numbers of immune cells to enhance engraftment of the human immune system was limited by the risk for graft-versus-host disease (GVHD) in this model.

In the present study, B cell engraftment was detected with marginal B cell numbers in the peripheral blood and less than expected B cells in the spleens of control mice. In α IL-21R-treated animals, B cell engraftment was negligible. It is known that the engraftment of B cells in humanized mouse models is challenging, as described by others.⁴⁰ One technical obstacle is the long maturation time of B cells after infusion, which can take up to five to six months after administration of human hematopoietic stem cells in mice.⁴¹ The model used in the present study does not allow such long engraftment times as after three months the risk for GVHD caused by human T cells that recognize mouse antigens rapidly increases.⁴² In addition, we have seen that infusion of higher splenocyte doses as well leads to an increased incidence of GVHD. In our study, infusion of α IL-21R at a later time point in order to diminish the effect of the IL-21R blockade on T and B cell repopulation is therefore an unsuitable option. An alternative might be to infuse mature B cells instead of the CD43- quiescent B cell population in order to accelerate the process of B cell activation and reconstitution.

As described above, T cells are necessary in the process of B cell expansion.⁴¹ Thus, a decreased T cell homeostatic proliferation caused by α IL-21R might lead to impairment of B cell reconstitution as we have seen in our model. Since we found an effect of α IL-21R on T and B cell engraftment within the host due to the effects of IL-21R signaling on homeostatic proliferation, blockade of this receptor may also impair maintenance of both arms of the immune system. The inhibition of allograft rejection through reduced engraftment of reconstituted immune cells by IL-21R blockade that we detected in our study is in line with a previous study by Oliveira et al.²⁵ In this study, cyclosporine-A and rapamycin were introduced in a similar humanized skin transplant mouse model which resulted in lower numbers of peripheral T cells combined with a decrease in T cell infiltration and inflammation of the human skin.²⁵ The humanized skin transplant model is also used to study the effect of regulatory T (Treg) cells on reducing rejection of human skin.^{23,24} These studies demonstrated that Treg cells might have an inhibiting effect on the engraftment of human lymphocytes. The effect of immune modulating compounds on the engraftment of lymphocytes forms the main limitation in this study. For future studies, local infusion of the compound into the transplanted skin may be an alternative to overcome the systemic effect of the immune modulating therapies on lymphocyte reconstitution.⁴³ In addition, the use of a reference drug alongside the α IL-21R compound during future experiments will further clarify the effectiveness of blockade of IL-21R signaling.

The humanized mouse model represented in this study forms a valuable preclinical model to evaluate human-specific reagents such as humanized monoclonal antibody therapies. However, since the infusion of these reagents might also affect the reconstitution of the infused human lymphocytes one should take into account that reduced rejection of the skin may occur as a result of the impaired engraftment of the human lymphocytes. In conclusion, we prove that

blockade of IL-21R signaling delays the start of rejection of a human skin graft, but also influences T and B cell reconstitution in Balb/c IL2 γ ^{-/-}Rag2^{-/-} mice. These preclinical data using an in vivo humanized system demonstrate significant promise for blockade of IL-21R signaling in transplantation.

Acknowledgments

We would like to thank Pfizer for supplying the anti-IL-21R antibody ATR-107 and D. Reijerkerk for the technical assistance during the experiments.

References

1. Coemans M, Süsal C, Döhler B, et al. Analyses of the short- and long-term graft survival after kidney transplantation in Europe between 1986 and 2015. *Kidney Int.* 2018;94(5):964-973.
2. Loupy A, Haas M, Solez K, et al. The Banff 2015 Kidney Meeting Report: Current Challenges in Rejection Classification and Prospects for Adopting Molecular Pathology. *Am J Transplant.* 2017;17(1):28-41.
3. Wiebe C, Gibson IW, Blydt-Hansen TD, et al. Rates and determinants of progression to graft failure in kidney allograft recipients with de novo donor-specific antibody. *Am J Transplant.* 2015;15(11):2921-2930.
4. Lefaucheur C, Loupy A, Vernerey D, et al. Antibody-mediated vascular rejection of kidney allografts: a population-based study. *Lancet.* 2013;381(9863):313-319.
5. Inaba A, Clatworthy MR. Novel immunotherapeutic strategies to target alloantibody-producing B and plasma cells in transplantation. *Curr Opin Organ Transplant.* 2016;21(4):419-426.
6. Spolski R, Leonard WJ. Interleukin-21: a double-edged sword with therapeutic potential. *Nat Rev Drug Discov.* 2014;13(5):379-395.
7. Asao H, Okuyama C, Kumaki S, et al. Cutting edge: the common gamma-chain is an indispensable subunit of the IL-21 receptor complex. *J Immunol.* 2001;167(1):1-5.
8. Nurieva R, Yang XO, Martinez G, et al. Essential autocrine regulation by IL-21 in the generation of inflammatory T cells. *Nature.* 2007;448(7152):480-483.
9. Parrish-Novak J, Dillon SR, Nelson A, et al. Interleukin 21 and its receptor are involved in NK cell expansion and regulation of lymphocyte function. *Nature.* 2000;408(6808):57-63.

10. Korn T, Bettelli E, Gao W, et al. IL-21 initiates an alternative pathway to induce proinflammatory T(H)17 cells. *Nature*. 2007;448(7152):484-487.
11. Tian Y, Zajac AJ. IL-21 and T Cell Differentiation: Consider the Context. *Trends Immunol*. 2016;37(8):557-568.
12. Xin G, Schauder DM, Lainez B, et al. A Critical Role of IL-21-Induced BATF in Sustaining CD8-T-Cell-Mediated Chronic Viral Control. *Cell Rep*. 2015;13(6):1118-1124.
13. Zeng R, Spolski R, Finkelstein SE, et al. Synergy of IL-21 and IL-15 in regulating CD8+ T cell expansion and function. *J Exp Med*. 2005;201(1):139-148.
14. Ozaki K, Spolski R, Feng CG, et al. A critical role for IL-21 in regulating immunoglobulin production. *Science*. 2002;298(5598):1630-1634.
15. Ozaki K, Spolski R, Ettinger R, et al. Regulation of B cell differentiation and plasma cell generation by IL-21, a novel inducer of Blimp-1 and Bcl-6. *J Immunol*. 2004;173(9):5361-5371.
16. Yan L, de Leur K, Hendriks RW, et al. T Follicular Helper Cells As a New Target for Immunosuppressive Therapies. *Front Immunol*. 2017;8:1510.
17. Shi X, Que R, Liu B, et al. Role of IL-21 signaling pathway in transplant-related biology. *Transplant Rev (Orlando)*. 2016;30(1):27-30.
18. Baan CC, Balk AH, Dijke IE, et al. Interleukin-21: an interleukin-2 dependent player in rejection processes. *Transplantation*. 2007;83(11):1485-1492.
19. de Graav GN, Dieterich M, Hesselink DA, et al. Follicular T helper cells and humoral reactivity in kidney transplant patients. *Clin Exp Immunol*. 2015;180(2):329-340.
20. de Leur K, Clahsen-van Groningen MC, van den Bosch TPP, et al. Characterization of ectopic lymphoid structures in different types of acute renal allograft rejection. *Clin Exp Immunol*. 2018;192(2):224-232.

21. de Leur K, Dor FJ, Dieterich M, et al. IL-21 Receptor Antagonist Inhibits Differentiation of B Cells toward Plasmablasts upon Alloantigen Stimulation. *Front Immunol.* 2017;8:306.
22. Hippen KL, Bucher C, Schirm DK, et al. Blocking IL-21 signaling ameliorates xenogeneic GVHD induced by human lymphocytes. *Blood.* 2012;119(2):619-628.
23. Issa F, Hester J, Goto R, et al. Ex vivo-expanded human regulatory T cells prevent the rejection of skin allografts in a humanized mouse model. *Transplantation.* 2010;90(12):1321-1327.
24. Landman S, de Oliveira VL, van Erp PEJ, et al. Intradermal injection of low dose human regulatory T cells inhibits skin inflammation in a humanized mouse model. *Sci Rep.* 2018;8(1):10044.
25. de Oliveira VL, Keijsers RR, van de Kerkhof PC, et al. Humanized mouse model of skin inflammation is characterized by disturbed keratinocyte differentiation and influx of IL-17A producing T cells. *PLoS One.* 2012;7(10):e45509.
26. Kenney LL, Shultz LD, Greiner DL, et al. Humanized Mouse Models for Transplant Immunology. *Am J Transplant.* 2016;16(2):389-397.
27. Vugmeyster Y, Allen S, Szklut P, et al. Correlation of pharmacodynamic activity, pharmacokinetics, and anti-product antibody responses to anti-IL-21R antibody therapeutics following IV administration to cynomolgus monkeys. *J Transl Med.* 2010;8:41.
28. Vugmeyster Y, Guay H, Szklut P, et al. In vitro potency, pharmacokinetic profiles, and pharmacological activity of optimized anti-IL-21R antibodies in a mouse model of lupus. *MAbs.* 2010;2(3):335-346.

29. Zhu M, Pleasic-Williams S, Lin TH, et al. pSTAT3: a target biomarker to study the pharmacology of the anti-IL-21R antibody ATR-107 in human whole blood. *J Transl Med*. 2013;11:65.
30. Juráňová J, Franková J, Ulrichová J. The role of keratinocytes in inflammation. *J Appl Biomed*. 2017;15(3):169-179.
31. Tian Y, Cox MA, Kahan SM, et al. A Context-Dependent Role for IL-21 in Modulating the Differentiation, Distribution, and Abundance of Effector and Memory CD8 T Cell Subsets. *J Immunol*. 2016;196(5):2153-2166.
32. Nguyen H, Weng NP. IL-21 preferentially enhances IL-15-mediated homeostatic proliferation of human CD28+ CD8 memory T cells throughout the adult age span. *J Leukoc Biol*. 2010;87(1):43-49.
33. Datta S, Sarvetnick NE. IL-21 limits peripheral lymphocyte numbers through T cell homeostatic mechanisms. *PLoS One*. 2008;3(9):e3118.
34. Nurieva RI, Chung Y, Hwang D, et al. Generation of T follicular helper cells is mediated by interleukin-21 but independent of T helper 1, 2, or 17 cell lineages. *Immunity*. 2008;29(1):138-149.
35. Vogelzang A, McGuire HM, Yu D, et al. A fundamental role for interleukin-21 in the generation of T follicular helper cells. *Immunity*. 2008;29(1):127-137.
36. Fröhlich A, Kisielow J, Schmitz I, et al. IL-21R on T cells is critical for sustained functionality and control of chronic viral infection. *Science*. 2009;324(5934):576-1580.
37. Yi JS, Du M, Zajac AJ. A vital role for interleukin-21 in the control of a chronic viral infection. *Science*. 2009;324(5934):1572-1576.

38. Zaitseu M, Issa F, Hester J, et al. Selective blockade of CD28 on human T cells facilitates regulation of alloimmune responses. *JCI Insight*. 2017;2(19).
39. Nadig SN, Wieckiewicz J, Wu DC, et al. In vivo prevention of transplant arteriosclerosis by ex vivo-expanded human regulatory T cells. *Nat Med*. 2010;16(7):809-813.
40. Seung E, Tager AM. Humoral immunity in humanized mice: a work in progress. *J Infect Dis*. 2013;208 (Suppl 2):S155-159.
41. Lang J, Kelly M, Freed BM, et al. Studies of lymphocyte reconstitution in a humanized mouse model reveal a requirement of T cells for human B cell maturation. *J Immunol*. 2013;190(5):2090-2101.
42. King MA, Covassin L, Brehm MA, et al. Human peripheral blood leucocyte non-obese diabetic-severe combined immunodeficiency interleukin-2 receptor gamma chain gene mouse model of xenogeneic graft-versus-host-like disease and the role of host major histocompatibility complex. *Clin Exp Immunol*. 2009;157(1):104-118.
43. Roemeling-van Rhijn M, Khairoun M, Korevaar SS, et al. Human Bone Marrow- and Adipose Tissue-derived Mesenchymal Stromal Cells are Immunosuppressive In vitro and in a Humanized Allograft Rejection Model. *J Stem Cell Res Ther*. 2013;Suppl 6(1):20780.

Figure legends

Figure 1.

STAT3 phosphorylation is effectively blocked by α IL-21R

(A) Schematic representation of the treatment strategy to measure blockade of IL-21R dependent STAT3 phosphorylation (STAT3p). Mice were adoptively transferred with 5×10^6 splenocytes plus 2.5×10^6 enriched quiescent B cells. α IL-21R was administered via intraperitoneal injection at a concentration of 10mg/kg at day 7, 14 and 21 after adoptive transfer of splenocytes. PBS was used as a vehicle control. Blood was sampled on days 28, 35, 42, 49, 56, and 62 after adoptive cellular transfer ($n=1$ per time point). (B) Typical example dot plots of STAT3p analysis of a vehicle-treated animal and a α IL-21R-treated animal. 42 days after adoptive cellular transfer blood was sampled and stimulated for 15 minutes with 100 ng/ml recombinant human IL-21, 100 ng/ml recombinant human IL-6 as a positive control, or not stimulated (unstim.). Subsequently, cells were stained for CD3, CD4 and STAT3p. Numbers within the dot plots indicate proportions of the STAT3p positive population. (C) Proportions of STAT3p of CD4⁺ T cells after stimulation with IL-21, IL-6, or control at different time points after adoptive cellular transfer and α IL-21R treatment. Before day 42, the human lymphocyte numbers in the blood were not sufficient for STAT3p measurements.

Figure 2.

α IL-21R mAb treatment delays rejection of human skin grafts

(A) Treatment strategy used to explore the effect of α IL-21R on rejection of human skin grafts. A circular piece of human skin with a diameter of 1 cm was stitched on the mouse (day -35). After 35 days the human skin was engrafted and mice then received 5×10^6 splenocytes with 2.5×10^6 enriched quiescent B cells (day 0). α IL-21R was administered at a concentration of

10mg/kg on days 7, 14 and 21 after adoptive cellular transfer ($n=8$ mice). PBS was used as a vehicle control ($n=7$ mice). 30 days after adoptive cellular transfer mice were sacrificed for cross-sectional analysis. (B) Hematoxylin and eosin (H&E) staining of the complete human skin graft of a vehicle-treated animal and an α IL-21R-treated animal. (C) 10x magnification of the H&E staining of the human skin graft of a vehicle and α IL-21R-treated animal. In the vehicle-treated animal (upper panel) thickening of the epidermis and dermal infiltrate was detected in contrast to the α IL-21R-treated animal (lower panel). (D) Quantified data of epidermal thickness. Epidermal thickness is presented in μm as a mean of twenty consecutive measurements with the standard error of the mean (SEM). Vehicle group $n=7$, α IL-21R group $n=8$. (* $p<0.05$).

Figure 3.

IL-21R blockade reduces lymphocyte infiltration in skin grafts

Typical examples of immunohistochemical stainings of human skin grafts for (A) human CD45, (B) human CD3, (C) human CD4, (D) human CD8, and (E) human CD20. Increased infiltration of human lymphocytes was detected in skin of vehicle-treated animals compared to α IL-21R-treated animals. Quantified data are presented as mean proportions of the positive area with SEM or as mean positive cells counted within the total dermis and epidermis with SEM.

Magnification: 10x. Vehicle group $n=7$, α IL-21R group $n=8$. (* $p<0.05$, *** $p<0.001$).

Figure 4.

IL21R blockade reduces human skin inflammation markers

(A) Immunohistochemistry for skin inflammation marker keratin 17 (Ker17). Typical example of the human skin graft of a vehicle-treated animal and an α IL-21R-treated animal are depicted combined with the quantified data. (B) Immunohistochemistry for proliferation marker Ki67. A typical example of the human skin graft of a vehicle-treated animal and an α IL-21R-treated

animal are depicted combined with the quantified data. Quantified data are presented as mean proportions of the positive area with SEM. Magnification: 10x. Vehicle group $n=7$, α IL-21R group $n=8$. (* $p<0.05$).

Figure 5.

α IL-21R mAb treatment affects human leukocyte engraftment

(A) Spleen weight in mg of mice treated following the schedule depicted in Figure 1A Mice were sacrificed on days 28, 35, 42, 49, 56, and 63 post adoptive cellular transfer. Two vehicle-treated animals were sacrificed on days 28 and 42 post adoptive cellular transfer. $n=1$ per time point. (B) Absolute numbers of CD45⁺ lymphocytes of mice treated following the schedule depicted in Figure 1A. Mice were sacrificed on days 28, 35, 42, 49, 56, and 63 post adoptive cellular transfer. One vehicle-treated animal was sacrificed on day 42 post adoptive cellular transfer. $n=1$ per time point. (C) Spleen weight in mg and proportions of CD45⁺ human lymphocytes of the total viable leukocytes in the spleen. Measurements were performed 30 days post adoptive cellular transfer (D) Proportions of human CD45⁺ lymphocytes within the total viable leukocytes within blood of the vehicle-treated animals versus the α IL-21R-treated animals 30 days after adoptive cellular transfer. A typical example of a dot plot from a vehicle-treated animal and an α IL-21R-treated animals is depicted on the right-hand side. (E) Proportions of CD3⁺ T cells and CD19⁺ B cells within human CD45⁺ lymphocytes in the blood. Vehicle-treated animals were compared to the α IL-21R-treated animals 30 days after adoptive cellular transfer. Vehicle group $n=7$, α IL-21R group $n=8$. (N.S. = not significant, * $p<0.05$, ** $p<0.01$, *** $p<0.001$).

Figure 1

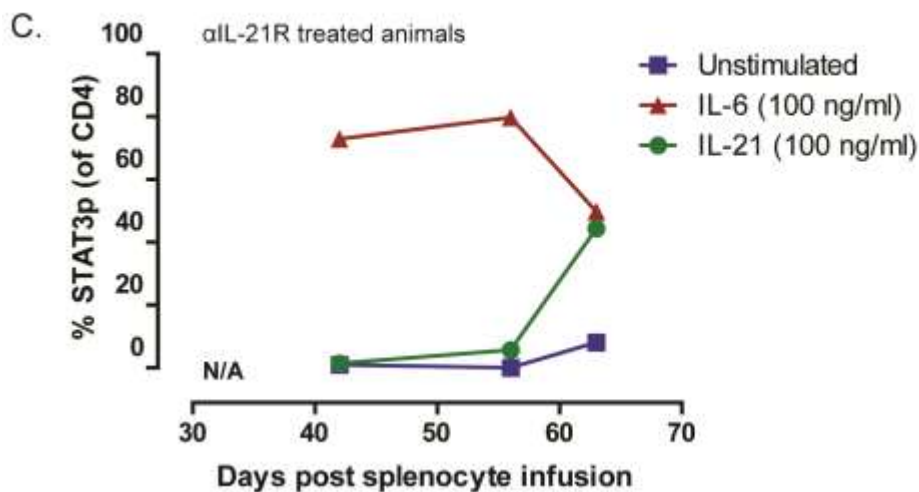
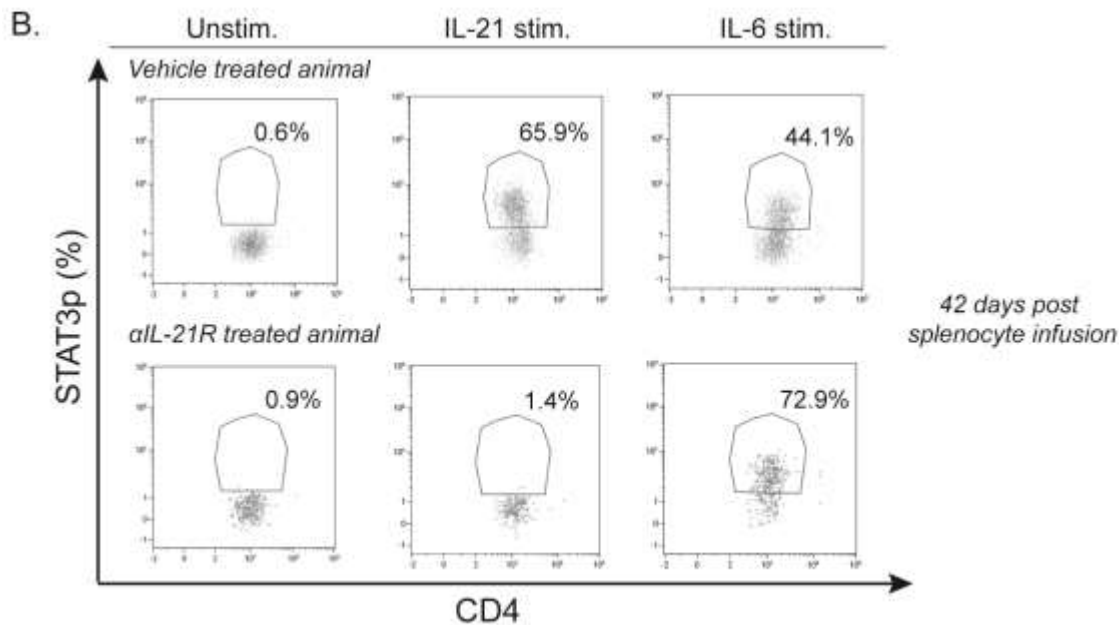
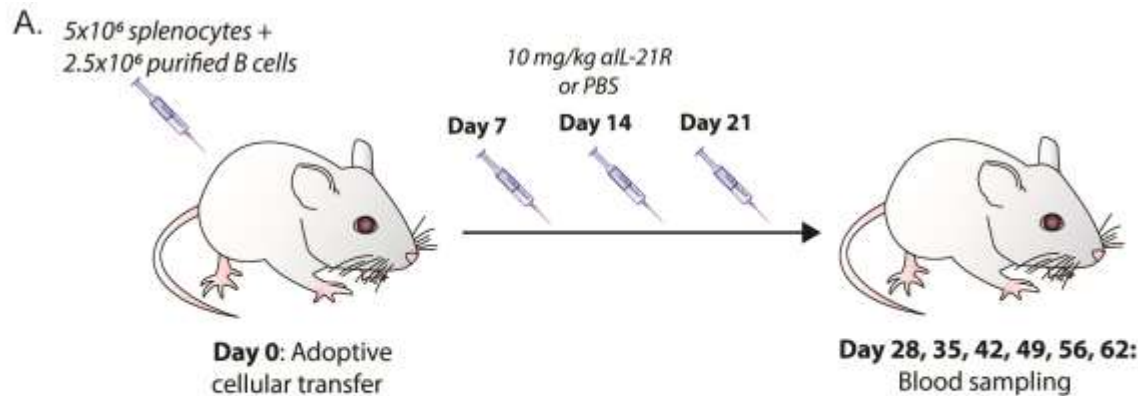


Figure 2

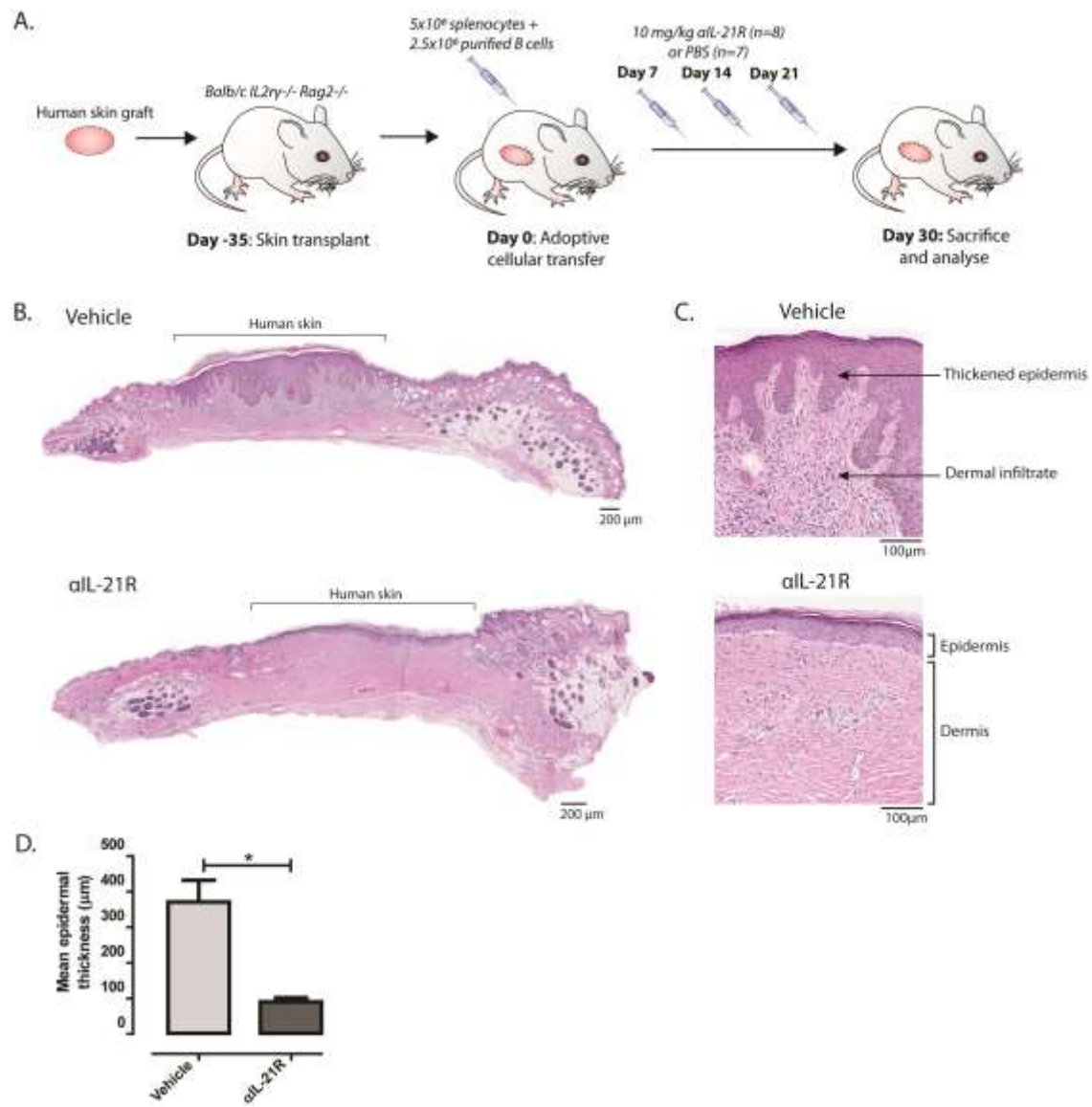


Figure 3

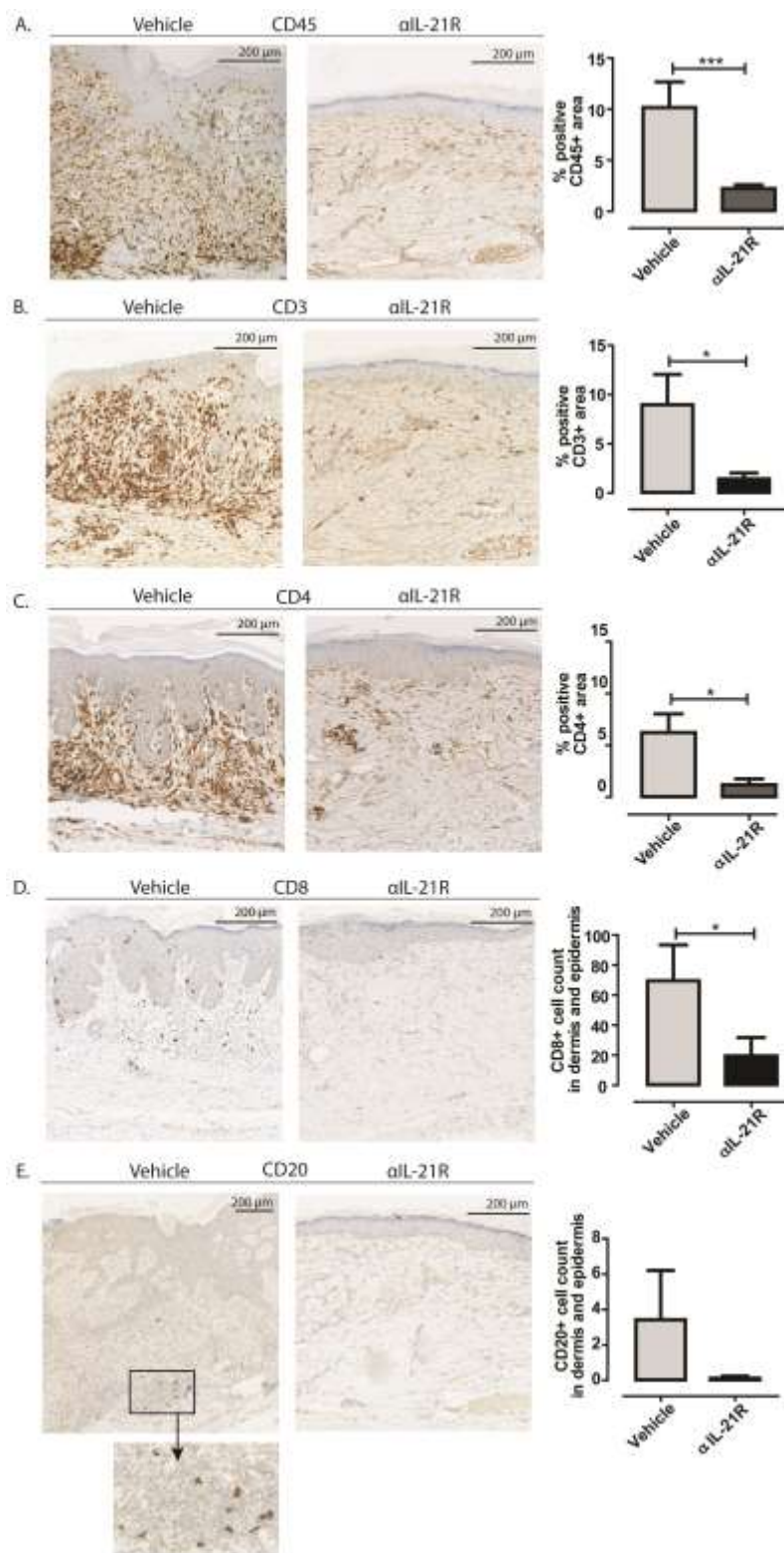


Figure 4

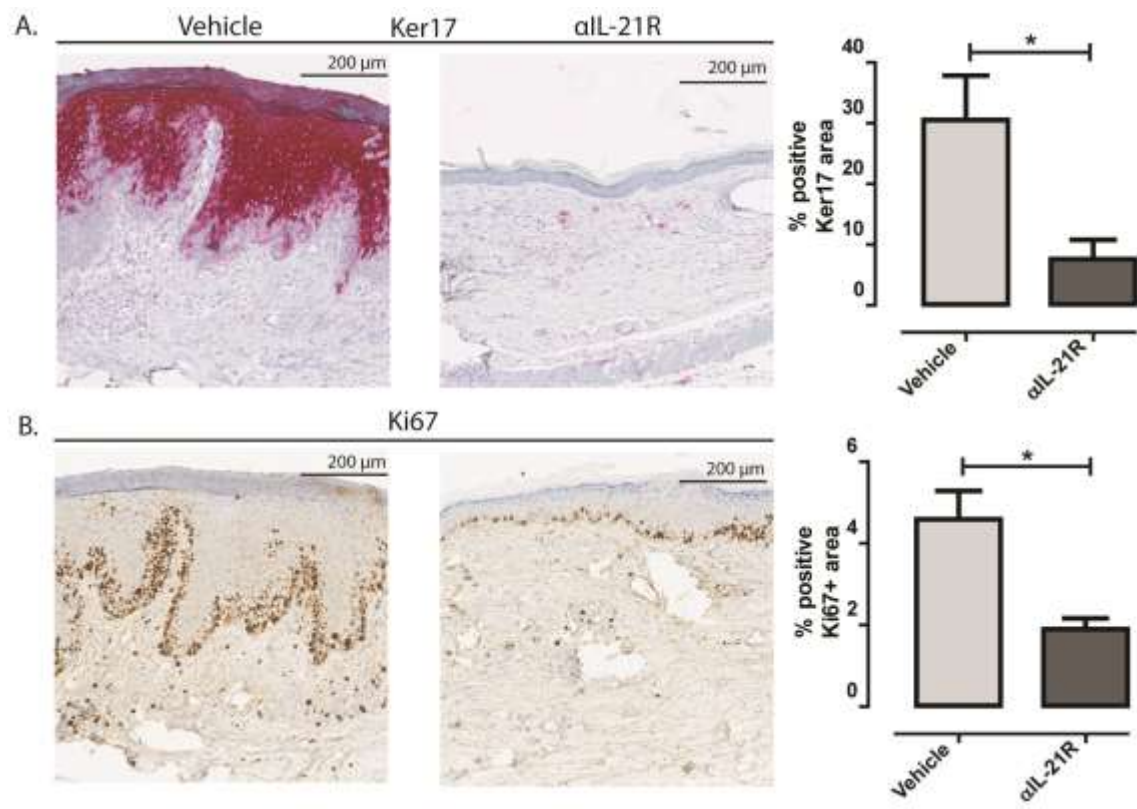


Figure 5

Figure 5.

